# Simultaneous Binding of Two Peptidyl Ligands by a Src Homology 2 Domain

Yanyan Zhang,[†,‡] Jinjin Zhang,[†,§,#] Chunhua Yuan,[∥] Ryan L. Hard,[†,‡] In-Hee Park,[⊥,@] Chenglong Li,[†,⊥,@] Charles Bell,[†,§] and Dehua Pei*[,†,‡]

[†]Ohio State Biochemistry Program, [‡]Department of Chemistry, [§]Department of Molecular and Cellular Biochemistry, [∥]Campus Chemical Instrument Center, [⊥]Chemical Physics Program, and [@]Division of Medicinal Chemistry, College of Pharmacy, The Ohio State University, 100 West 18th Avenue, Columbus, Ohio 43210, United States

**S** Supporting Information

**ABSTRACT:** Src homology 2 (SH2) domains mediate protein−protein interactions by recognizing phosphotyrosine (pY)-containing sequences of target proteins. In all of the SH2 domain−pY peptide interactions described to date, the SH2 domain binds to a single pY peptide. Here, determination of the cocrystal structure of the N-terminal SH2 domain of phosphatase SHP-2 bound to a class IV peptide (VIpYFVP) revealed a noncanonical 1:2 (protein−peptide) complex. The first peptide binds in a canonical manner with its pY side chain inserted in the usual binding pocket, while the second pairs up with the first to form two antiparallel β-strands that extend the central β-sheet of the SH2 domain. This unprecedented binding mode was confirmed in the solution phase by NMR experiments and shown to be adopted by pY peptides derived from cellular proteins. Site-directed mutagenesis and surface plasmon resonance studies revealed that the binding of the first peptide is pY-dependent, but phosphorylation is not required for the second peptide. Our findings suggest a potential new function for the SH2 domain as a molecular clamp to promote dimerization of signaling proteins.
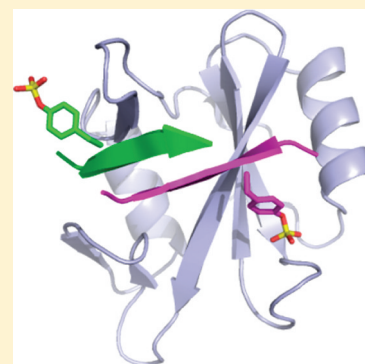
The Src homology 2 (SH2) domain is a small protein module consisting of ∼100 amino acids. It was first identified in the N-terminal regions of Src family protein tyrosine kinases and subsequently found in >100 human proteins, many of which are involved in intracellular signaling processes.[1] SH2 domains recognize specific phosphotyrosyl (pY) residues in their partner proteins, promoting protein−protein interactions. The sequence specificity of an SH2 domain−pY protein interaction is primarily determined by the pY residue and the three or four residues immediately C-terminal to pY,[2,3] although some SH2 domains require a more extended region of the pY peptide for high-affinity and -specificity interactions.[4−8] The structural basis for the specific interaction has been very well studied.[9−14] A key interaction, which is common to all SH2 domains, is the insertion of the pY side chain into a deep pocket in the SH2 domain, where an invariant arginine residue (Arg βB5) forms a bidentate interaction with the pY phosphate group. Additional binding energy is provided by interactions between amino acids adjacent to pY, particularly the three residues immediately C-terminal to pY, and the less conserved surface of the SH2 domain. This latter interaction also governs the selectivity of a given SH2 domain in binding to a specific pY partner.

SHP-2 is a nontransmembrane protein tyrosine phosphatase (PTP) that contains two N-terminal SH2 domains and a C-terminal catalytic domain.[15] In the absence of any pY ligand, SHP-2 exists in an inactive conformation, with its N-terminal SH2 domain occluding the substrate-binding pocket of the PTP

domain.[16] Occupation of the N-SH2 domain with a pY-containing ligand leads to release of the inhibitory N-SH2−PTP interaction and subsequent activation of the enzyme.[17,18] The N-terminal SH2 domain of SHP-2 thus acts as a molecular switch that controls both the specificity and the activity of the enzyme. The sequence specificity of both SH2 domains has previously been determined using combinatorial libraries.[6,7] Unlike the classical SH2 domains, SHP-2 SH2 domains require more extended sequences both N- and C-terminal to the pY residue (positions pY − 2 to pY + 5) for high-affinity binding. The C-SH2 domain binds pY peptides of a single consensus sequence (T/V/I/y)XpY(A/s/t)X(I/V/L) (where X is any amino acid and the lowercase letters represent less preferred residues). On the other hand, the N-SH2 domain of SHP-2 can recognize four distinct classes of sequences (classes I−IV), with consensus sequences of (I/L/V/m)XpY(T/V/A)X(I/V/L/f), W(M/T/v)pY(y/r)(I/L)X, (I/V)XpY(L/M/T)Y(A/P/T/S/g), and (I/V/L)XpY(F/M)XP, respectively.[6] X-ray crystal structures of the SHP-2 N-SH2 domain in complex with the class I peptides have been reported.[12] To further investigate the structural basis for recognition of the four different classes of peptide ligands, we attempted to determine the structures of the SHP-2 N-SH2 domain bound to peptides from class I (RLNpYAQLWHR), class III (RIHpYLYALNR), and class IV

(RVIpYFVPLNR) by X-ray crystallography. We show that the mode of binding of the SHP-2 N-SH2 domain with class I ligands closely matches that of a high-affinity complex between the N-SH2 domain and a class I peptide derived from the platelet-derived growth factor receptor (VLpY[1009]TAV).[12] In contrast, the class IV ligand bound to the SH2 domain as an antiparallel dimer, which was confirmed by solution-phase NMR studies. To the best of our knowledge, this is the first example of a single SH2 domain binding to two pY ligands, thus expanding the functional implications of SH2−peptide interactions.

## ■ EXPERIMENTAL PROCEDURES

**Materials.** Antibiotics, Sephadex G-25 resin, and organic solvents were obtained from Sigma-Aldrich (St. Louis, MO). Talon resin for IMAC purification was purchased from Clontech (Mountain View, CA). The Q-Sepharose Fast-Flow column and thrombin were purchased from Amersham (Pittsburgh, PA). Reagents for peptide synthesis were from Advanced ChemTech (Louisville, KY), Peptides International (Louisville, KY), and NovaBiochem (La Jolla, CA). Protein concentrations were determined by the Bradford method using bovine serum albumin as a standard.

**Expression and Purification of the SHP-2 N-SH2 Domain.** Plasmid pET28a-SHP2-NSH2, which encodes the N-SH2 domain of SHP-2 (amino acids 1−106) and an N-terminal six-histidine tag, had previously been described.[6] *Escherichia coli* BL21(DE3) cells harboring this plasmid were grown in LB medium supplemented with 0.1 mg/mL ampicillin at 37 °C. When the $OD_{600}$ value reached 0.6, the cells were induced by the addition of 0.1 mM isopropyl β-D-thiogalactoside and allowed to grow for an additional 4 h at 30 °C. The cells were harvested by centrifugation and resuspended in 20 mL (for 1 L of cell culture) of Talon column buffer [50 mM sodium phosphate (pH 7.8), 500 mM NaCl, and 5 mM imidazole] containing protease inhibitors (1 mM PMSF, 10 μg/mL trypsin inhibitor, and 1 μM pepstatin A), lysozyme (1 mg/mL), and protamine sulfate (5 mg/mL). After incubation for 30 min at 4 °C, the mixture was sonicated briefly. The crude lysate was centrifuged at 13000g for 20 min, and the supernatant was loaded onto a Talon column (2 cm × 10 cm containing 20 mL of resin) that had been equilibrated in Talon column buffer. The column was washed with Talon column wash buffer [50 mM sodium phosphate (pH 7.8), 500 mM NaCl, and 25 mM imidazole] and eluted with a buffer containing 50 mM sodium phosphate (pH 7.8), 500 mM NaCl, and 125 mM imidazole. The purified SH2 protein was concentrated to a volume of ∼20 mL with Amicon Ultra-15 centrifugal filter units (Millipore). Buffer exchange and removal of the six-histidine tag were achieved simultaneously by adding 200 units of thrombin (GE healthcare) into the dialysis bag and dialyzing overnight against 2 L of buffer A [25 mM Tris (pH 8.0) and 20 mM NaCl] at room temperature. The resulting digested protein sample was passed through the Talon column again to remove any uncleaved protein. The flow-through fraction was collected and loaded onto Q-Sepharose column (2 cm × 10 cm) equilibrated in buffer A. The column was eluted with buffer A containing a linear gradient of 0 to 500 mM NaCl. The fractions containing the pure SHP-2 N-SH2 protein (as judged by sodium dodecyl sulfate−polyacrylamide gel electrophoresis) were pooled and concentrated to >10 mg/mL by Amicon Ultra-15 centrifugal filter units. The concentrated

protein was dialyzed against 10 mM Mes (pH 5.5) and 50 mM KCl. After the addition of 0.5 mM tris(carboxyethyl)phosphine, the protein solution was flash-frozen in a 2-propanol/dry ice bath and stored at −80 °C.

**Preparation of the [$^{15}$N]SHP-2 N-SH2 Domain.** *E. coli* BL21(DE3) cells harboring the DNA construct described above were cultured in M9 minimal medium [prepared with ($^{15}$NH$_4$)$_2$SO$_4$] supplemented with 0.4% (w/v) glucose, 5 mM MgSO$_4$·7H$_2$O, 10 μM FeSO$_4$·7H$_2$O, and 0.01% thiamine at 37 °C to an $OD_{600}$ of 0.7. The cells were induced with 0.1 mM isopropyl β-D-thiogalactoside at 20 °C for 15 h and harvested by centrifugation. Cell lysis and purification by metal affinity chromatography on the Talon column were performed as described above. The elution buffer was exchanged into an appropriate NMR buffer by dialysis against 20 mM sodium phosphate (pH 7.4), 150 mM NaCl, and 1 mM dithiothreitol [for two-dimensional (2D) $^1$H−$^{15}$N heteronuclear single-quantum correlation (HSQC) and $^1$H−$^{13}$C HSQC experiments] or 50 mM Hepes (pH 7.4) and 150 mM NaCl (for $^{31}$P NMR spectroscopy). The protein solution was lyophilized overnight and stored at −80 °C. Protein concentrations were determined by both the Bradford method using bovine serum albumin as a standard and measuring its absorbance at 280 nm (the two methods gave values that were within 10% of each other).

**Peptide Synthesis.** Peptides were synthesized on CLEAR-amide resin (0.4 mmol/g) using standard Fmoc/HBTU chemistry. After cleavage and side chain deprotection with a modified reagent K (6.5% phenol, 5% water, 5% thioanisole, 2.5% ethanedithiol, and 1% anisole in trifluoroacetic acid), the peptides were precipitated with cold ether and purified by reversed-phase HPLC on a C$_{18}$ column (Varian 120 Å, 4.6 mm × 250 mm). The identities of the peptides were confirmed by MALDI-TOF mass spectrometric analyses. The peptides used for $^{13}$C−$^1$H HSQC experiments were acetylated with ($^{13}$CH$_3$CO)$_2$O at the N-termini. Peptides used for surface plasmon resonance (SPR) studies were biotinylated at their N-termini by treatment with *N*-hydroxysuccinimido-biotin (Sigma). The concentrations of the peptides were determined by a quantitative ninhydrin test or their absorbance at 280 nm (for peptides that contained tyrosine in their sequences). For the peptides used in $^{15}$N−$^1$H and $^{13}$C−$^1$H HSQC experiments, the concentration was confirmed by various methods, including direct weighing, ninhydrin tests, absorbance increase at 280 nm upon phosphatase treatment, and one-dimensional (1D) $^1$H NMR (Figure S1 of the Supporting Information).

**Crystallization and Data Collection.** The purified N-terminal SH2 domain of SHP-2 was cocrystallized with peptides RVIpYFVPLNR (termed pYFVP hereafter), RLNpYAQLWHR (termed pYAQL), and RIHpYLYALNR (termed pYLYA) at room temperature by hanging drop vapor diffusion. The SH2 domain (10 mg/mL) in 0.1 M Mes (pH 5.5) and 50 mM KCl was mixed with a slight molar excess of peptide (1.1 equiv) dissolved in water. The hanging drops were prepared by mixing 2 μL of the complex and 2 μL of the reservoir solution, which consisted of 20% PEG 3350, 0.1 M bis-Tris (pH 5.5), and 0.2 M Li$_2$SO$_4$. Large tetragonal crystals grew within approximately 3 days. Crystals were transferred to a cryo-protectant solution containing the reservoir solution supplemented with 20% glycerol and frozen in liquid nitrogen. The diffraction data were collected at −180 °C on beamline

19BM of the Advanced Photon Source. Data were integrated and scaled with DENZO/SCALEPACK.[19]

**Structure Determination.** The structure was determined by molecular replacement with MOLREP of the CCP4 suite[20] using the structure of the free SHP-2 N-SH2 domain [Protein Data Bank (PDB) entry 1AYD][12] as the search model. The structures with the pYFVP and pYAQL peptides were refined to 1.80 and 2.05 Å, respectively, using Refmac of the CCP4 suite.[20] After the first round of refinement, the electron density maps revealed strong density for two molecules of the pYFVP peptide and one molecule of the pYAQL peptide, which were built into the models. For pYLYA, no density corresponding to the peptide was observed. Several rounds of refinement with Refmac and model building using COOT[21] led to final models. The final refined SH2 domain−pYFVP structure consists of residues 4−103 of the SH2 domain (chain A), residues −2 to 4 of the first peptide (peptide A), and residues −2 to 3 of the second peptide (peptide B). The final SH2 domain−pYAQLW structure consists of residues 5−103 of the protein and residues −2 to 4 of the peptide (chain B). Side chains of residues, Arg4, LysBC1, and LysBG7 in the complex with pYFVP and Arg5, LysBC1, LysBG5, and LysBG7 in the complex with pYAQL, were not resolved in the electron density and were truncated to alanine. The C-terminal peptide residues, Arg6 and Asn5 of each peptide and Leu4 of peptide B in the complex with pYFVP and His5 and Arg6 of the peptide in the pYAQLW complex, were not observed in the electron density and were not included in the final structures. Data collection and refinement statistics are listed in Table 1. Structural figures were prepared using PYMOL (PyMOL Molecular Graphics System, Schrödinger, LLC, New York, NY). The secondary structural elements are defined using the Dali server[22] and named according to the nomenclature established previously for SH2 domains.[11,12] Solvent accessible surface area calculation was performed using the AREAIMOL feature of CCP4 with a probe radius of 1.4 Å.[20]

**NMR Spectroscopy.** Unless stated otherwise, data were recorded at room temperature on a Bruker DMX-600 spectrometer equipped with a TXI probe and three-axis gradients, and standard Bruker pulse sequences were used. The $^{15}$N-lableled SHP-2 N-SH2 domain was prepared in 500 μL of NMR buffer [20 mM sodium phosphate (pH 7.4), 150 mM NaCl, and 1 mM dithiothreitol] to give a final concentration of 0.46 mM in a 90% $H_2O$/10% $D_2O$ mixture. For two-dimensional $^1$H−$^{15}$N HSQC experiments, the protein sample was titrated with peptides to reach protein:peptide ratios of 1:0.5, 1:1, 1:1.5, 1:2, and 1:2.5. Three-dimensional (3D) $^{15}$N-edited NOESY-HSQC (200 ms NOE mixing time) and 3D $^{15}$N-edited TOCSY-HSQC (60 ms DIPSI-2 mixing time) spectra were recorded prior to and at the end of peptide titration. Two-dimensional $^1$H−$^{13}$C HSQC experiments were conducted by titrating 200 μM $^{13}$C-labeled peptide with 50, 100, and 150 μM SHP-2 N-SH2 domain to reach protein:peptide ratios of 0.25:1, 0.5:1, and 0.75:1, respectively. $^{31}$P NMR experiments were conducted on the Bruker DMX-600 spectrometer equipped with a BBO probe by titrating 300 μM peptide in Hepes buffer [50 mM Hepes and 150 mM NaCl (pH 7.4)] with various amounts of SHP-2 N-SH2 domain to reach targeted protein:peptide ratios.

**Affinity Measurement by SPR.** All measurements were taken at room temperature on a BIAcore 3000 instrument, using the N-terminal histidine-tagged SHP-2 N-SH2 domain.

**Table 1. Crystallographic and Refinement Statistics**

| | N-SH2−pYFVP | N-SH2−pYAQL |
|---|---|---|
| *X-ray Diffraction Data* | | |
| space group | $P4_32_12$ | $P4_32_12$ |
| unit cell dimensions | | |
| $a = b$ (Å) | 62.9 | 62.7 |
| $c$ (Å) | 75.3 | 75.3 |
| resolution (Å) | 48.3−1.8 (1.89−1.80) | 48.2−2.05 (2.13−2.05) |
| no. of unique reflections | 15827 | 9943 |
| redundancy | 11.2 (11.6) | 10.9 (11.3) |
| completeness (%) | 99.3 (100) | 99.0 (100) |
| $I/\sigma$ | 61.5 (5.0) | 46.5 (6.7) |
| $R_{merge}$ | 0.030 (0.382) | 0.064 (0.364) |
| *Refinement Statistics* | | |
| resolution (Å) | 48.3−1.80 | 48.2−2.05 |
| no. of reflections | 13727 | 9354 |
| $R_{work}/R_{free}$ | 0.197/0.216 | 0.193/0.234 |
| no. of non-hydrogen atoms | 992 | 860 |
| mean $B$ factor (Å$^2$) | 25.4 | 25.9 |
| root-mean-square deviation for bond lengths (Å) | 0.021 | 0.025 |
| root-mean-square deviation for bond angles (deg) | 1.96 | 2.10 |
| Ramachandran plot | | |
| favored regions | 98 (97.0%) | 95 (96.0%) |
| allowed regions | 3 (3.0%) | 4 (4.0%) |

Peptide biotin-(miniPEG)$_2$-RVIYFVPLNR-NH$_2$ was immobilized onto a streptavidin-coated sensorchip. The peptide was dissolved in HBS-EP buffer [10 mM Hepes, 150 mM NaCl, 3 mM EDTA, and 0.005% polysorbate 20 (pH 7.4)] to a final concentration of 17 μM and passed over the streptavidin chip until no further response unit increase was observed. The immobilized peptide was exposed to HBS-EP solutions containing a fixed concentration of the SH2 domain (10 μM) and increasing concentrations of pY peptide H$_2$N-(miniPEG)$_2$-VIpYFVPLNYRR-NH$_2$ (0−60 μM). Each solution was passed over the sensorchip for 2 min at a flow rate of 15 μL/min. The equilibrium response unit (RU$_{eq}$) for each pY peptide concentration was obtained by subtracting the response of the blank flow cell (which had no immobilized peptide) from that of the sample cell. To prepare the surface for the next run, the sensorchip was washed with a solution containing 0.05% SDS, 200 mM NaCl, and 10 mM NaOH for 30 s at a flow rate of 100 μL/min. The apparent dissociation constant ($K_{Dapp}$) was determined by nonlinear regression fitting of the data to the following equation:

$$RU_{eq} = (RU_{max}[pY])/(K_{Dapp} + [pY])$$

where RU$_{max}$ is the maximum response unit.

For competition studies, peptide NH$_2$-RLNpYAQLWHR-NH$_2$ was immobilized onto a CM5 chip at the N-terminal amine. Briefly, 50 μL of 0.4 M 1-ethyl-3-[3-(dimethylamino)-propyl]carbodiimide in ddH$_2$O was mixed with 50 μL of 0.1 M N-hydroxysuccinimide in ddH$_2$O and passed through the

desired channel at a flow rate of 10 $\mu$L/min. Next, the pY peptide (30 $\mu$g/mL) in the HBS-EP buffer was passed through the channel at a rate of 5 $\mu$L/min until a response unit increase of 200 RU was reached. Any excess reactive groups on the surface were quenched by passing 50 $\mu$L of 1 M ethanolamine (pH 8.5) over the surface at a rate of 5 $\mu$L/min. Competing peptides at concentrations ranging from 0.25 to 80 $\mu$M were incubated with 0.4 $\mu$M SHP-2 N-SH2 domain for 10 min and passed over the chip at a rate of 15 $\mu$L/min. The $RU_{eq}$ values were plotted against the competing peptide concentration, and the $IC_{50}$ values (concentration of competing peptide at which the $RU_{eq}$ value was reduced by 50%) were estimated from the curves.

## ■ RESULTS

**Crystal Structures of the SHP-2 N-SH2 Domain in Complex with Class I and IV Peptides.** To understand the structural basis for the ability of SHP-2 N-SH2 domain to recognize multiple classes of pY ligands, we attempted to determine the crystal structures of the SH2 domain in complex with representative class I, III, and IV ligands previously selected from a peptide library (peptides pYAQL, pYLYA, and pYFVP, respectively). In all three structures, the protein exhibits a typical SH2 domain fold consisting of a central antiparallel $\beta$-sheet flanked by two $\alpha$-helices, one on either side. The electron density map of the SH2 domain−pYLYA complex showed density for a phosphate ion in the expected pY-binding pocket, but no density for the rest of the peptide. The structure of the SH2 domain is nearly identical to the unbound SH2 domain structure previously reported (PDB entry 1AYD).[12] The electron density map for the SH2 domain−pYAQL complex allowed tracing of residues LNpYAQLW of the peptide, but the side chains of residues Gln(pY+2) and Trp(pY +4), which face out into solvent, were not resolved. The complex with the pYAQL peptide is very similar to the previous SH2 domian−peptide complexes (PDB entries 1AYA, 1AYB, and 1AYC) and will not be discussed in detail here.

The electron density map for the complex with the pYFVP peptide, however, is surprisingly different (Figure 1A). In contrast to all previous SH2 domain−peptide complexes, which contain a single peptide per SH2 domain, we observe two copies of the pYFVP peptide bound to the peptide-binding surface on the SHP-2 N-SH2 domain. This was the case for all three of the data sets that we collected on three different crystals. The 1:2 binding mode was observed consistently, despite the fact that only a slight molar excess of the peptide (1.1 equiv) was present during crystallization. The first peptide, peptide A, binds in a canonical manner, as an extended $\beta$-strand that pairs with strand $\beta$D of the SH2 domain and inserts its pY residue into a positively charged pocket formed in part by Arg$\beta$B5 and Lys$\beta$D6 (Figure 1B). The second peptide, peptide B, binds in an extended conformation running antiparallel to peptide A (Figure 1C). Residues IpYF of peptide B pair up with residues 88−90 of the BG loop of the SH2 domain, which form a short $\beta$-strand. Overall, the two peptides and the two short strands of the SH2 domain form an antiparallel four-stranded $\beta$-sheet, which adds onto the central four-stranded $\beta$-sheet ($\beta$A, $\beta$B, $\beta$C, and $\beta$D) of the SH2 domain to form a twisted eight-stranded $\beta$-sheet that almost forms a closed barrel.

The pY residue of peptide B is exposed on the surface of the structure, but forms a potentially favorable electrostatic interaction with LysBG5, whose $\varepsilon$-amino group is located 2.8
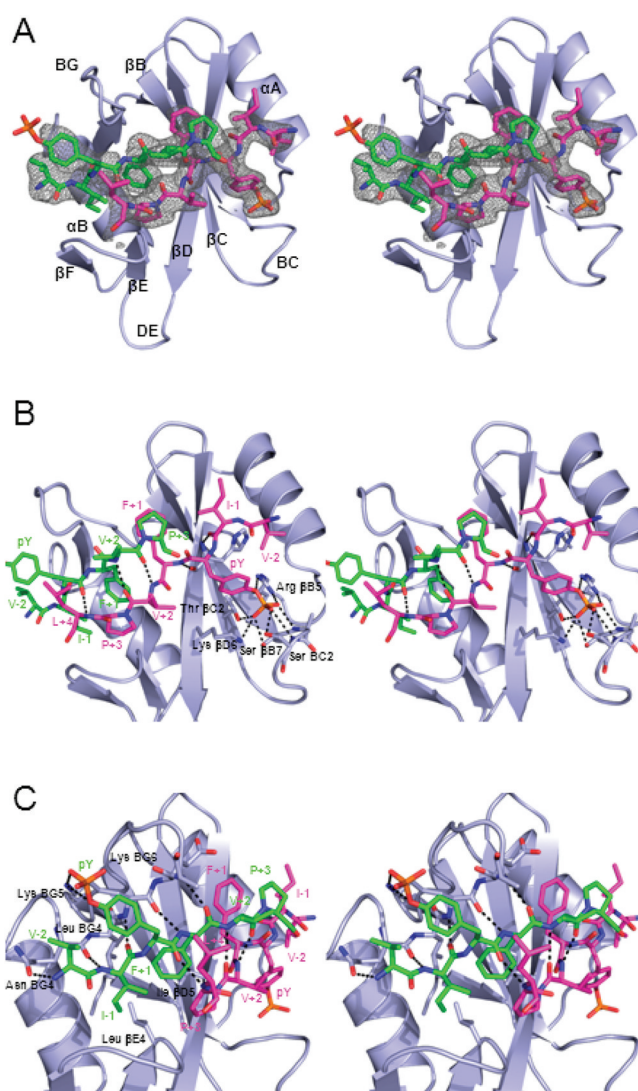


**Figure 1.** Crystal structure of the SHP-2 N-SH2 domain in complex with two pYFVP peptides. (A) Stereo ribbon diagram of the complex with the peptides shown in stick form. Peptide A, which binds in a canonical manner, is colored magenta and peptide B green. The final $2F_{obs} − F_{calc}$ electron density map calculated with model phases is contoured around the peptides. (B) Close-up stereoview of interactions of peptide A. Hydrogen bonds are shown as dashed lines. Peptides A and B pair up in an antiparallel manner to form three $\beta$-sheet hydrogen bonds. (C) Close-up stereoview of interactions involving peptide B, which forms four parallel $\beta$-sheet hydrogen bonds with the BG loop. The Phe2 residue of peptide B is buried in a hydrophobic pocket formed by Leu$\beta$E4, LeuBG4, Ile$\beta$D5, and Pro3 of peptide A. The pY residue of peptide B is mostly solvent exposed but forms a loose ion pair with LysBG5.

Å from the phosphate in the refined structure. The side chain of LysBG5, which was not at all resolved in the structures of the unbound SH2 domain or the complex with peptide pYAQL, is partially ordered in this structure. However, the electron density for the phosphate of peptide B, which is predominantly exposed, is considerably weaker than that for the buried phosphate of peptide A, suggesting that the former is likely to be flexible (Figure 1A). Accordingly, the average temperature factors for the phosphate atoms of peptides A and B are 47.8 and 68.2 $\text{Å}^2$, respectively. Thus, although there is the potential for a weak ion pair, the absence of tight interactions with the

phosphate of peptide B suggests that peptide B need not to be phosphorylated to form the 1:2 complex.

In addition to the hydrogen bonding interactions, binding of the two peptides is also stabilized by their hydrophobic interactions with the SH2 domain and with one another (Figure 1B,C). In particular, the side chain of Phe(pY+1) of peptide B is anchored into a hydrophobic pocket formed by the side chains of Ileβ D5, Leuβ E4 and LeuBG4 of the SH2 domain, and Pro3 of peptide A (Figure 1C). In the canonical SH2 domain−pY peptide structures, this hydrophobic pocket typically interacts with the nonpolar side chain of the pY + 3 residue. The side chains of Ile(pY−1) of peptide B and Phe(pY+1) of peptide A are also partially buried, although their interactions appear to be less optimal because they are less tightly packed (Figure 1C). Because of the antiparallel configuration, the Pro at the pY + 3 position of peptide A stacks closely over the pY + 1 Phe side chain of peptide B, and vice versa, to form additional hydrophobic interactions that appear to stabilize the complex. The side chains of the pY + 2 valine residues of both peptides are exposed at the surface of the complex but could form stabilizing hydrophobic interactions with each other, although they are not tightly packed (Figure 1B). On the basis of the structure, it appears that hydrophobic interactions between the FVP residues of the two peptides with one another and with the SH2 domain are in large part responsible for the specificity of the FVP sequence for the SHP-2 N-SH2 domain.

As seen previously in structures of the N-SH2 domain of SHP-2,[12] the peptide-binding surface appears as a wide groove that extends perpendicular to the plane of the central β-sheet of the SH2 domain. To accommodate peptide B of the pYFVP complex, the BG loop of the SH2 domain moves up and away from the peptide-binding site by ∼4 Å, as compared to the structure of this domain alone (Figure 2). In addition, the residues C-terminal to the pY of peptide A are pushed down to create room for the C-terminal residues of peptide B to bind. Consistent with the wider peptide-binding groove, these movements result in a significantly increased binding surface area in the pYFVP structure as compared to the pYAQL or previously published SH2 domain structures. A total of 670.6 Å$^2$ of solvent-accessible surface area of the SH2 domain is buried at the SH2 domain−pYFVP interface, which is contributed approximately equally by the two peptides, while a total of 417.7 Å$^2$ of surface area of the protein is buried at the SH2 domain−pYAQL interface.

**Observation of the 1:2 SH2 Domain−Peptide Complex in Solution by NMR.** To determine if the 1:2 complex observed crystallographically also exists in solution, we initially attempted to determine the stoichiometry of the SH2 domain−pY peptide complex by isothermal titration calorimetry. The experiment was unsuccessful because of the very small amount of heat released, consistent with the observation described above that hydrophobic interactions are largely responsible for complex formation. We therefore examined the SH2 domain−pYFVP complex by NMR spectroscopy. 2D $^1$H−$^{15}$N HSQC NMR spectroscopy of the uniformly $^{15}$N-labeled SHP-2 N-SH2 domain revealed good chemical shift dispersion of the backbone amides (Figure 3), indicative of a well-folded conformation in the free form. A few well-separated cross-peaks were tentatively assigned on the basis of sequence alignment and spectral similarity to that of the Grb2 SH2 domain.[23] The assignments were supported by the 3D $^{15}$N-
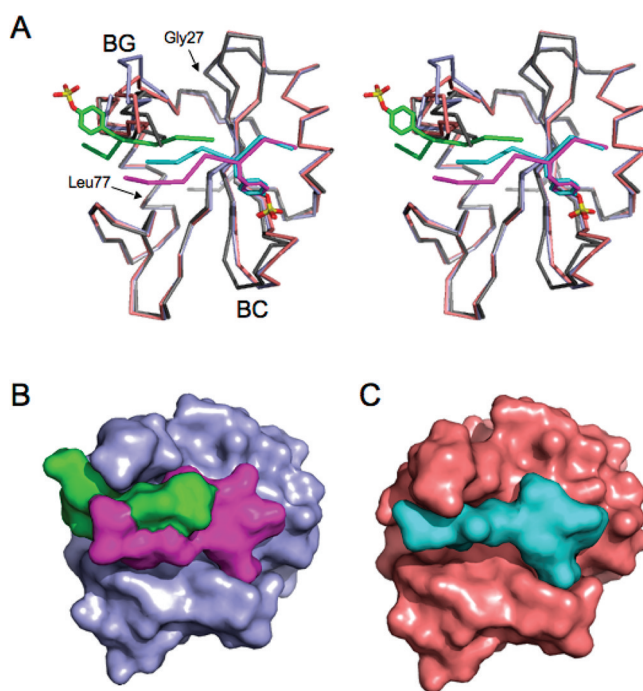


**Figure 2.** Conformational changes in the SHP-2 N-SH2 domain upon peptide binding. (A) Superposition of the unbound SH2 domain (gray), the complex with pYFVP peptides (light blue, cyan, and green), and the complex with the pYAQL peptide (salmon and cyan). The BG loop moves up to accommodate the AQLW peptide and even further up to accommodate the two pYFVP peptides. Smaller conformational changes occur for the BC loop, which is the same for both complexes. (B) Surface view of the SHP-2 SH2 domain−pYFVP complex. (C) Surface view of the SHP-2 SH2 domain−pYAQL complex. Comparison of panels B and C shows how the binding groove on the SH2 domain opens up to accommodate the two pYFVP peptides.

edited NOESY-HSQC and TOCSY-HSQC studies. For instance, in the TOCSY spectrum, Trp6 H$^{ε1}$ displays a cross-peak at 7.38 ppm that could be assigned to Trp6 H$^{δ1}$, whereas Gly27 H$^N$ exhibits two cross-peaks at 4.01 and 3.45 ppm, presumably attributed to its H$^{α1}$ and H$^{α2}$ atoms, respectively. Furthermore, Gly27 H$^N$ in the NOESY spectrum shows medium-sized NOEs to the resonances of 3.03 and 2.69 ppm, which naturally fall into the chemical shift range expected for H$^{β1}$ and H$^{β2}$ of the preceding residue, Asp26.

The $^{15}$N-labeled SH2 protein was then titrated with increasing concentrations of the pYFVP peptide, and the 2D $^1$H−$^{15}$N HSQC spectra were recorded at protein:peptide ratios of 1:0.5, 1:1, 1:1.5, 1:2, and 1:2.5. Addition of the peptide shifted a significant fraction of the cross-peaks, including those of Trp6 H$^{δ1}$ and Leu77 H$^N$, which are remote from the peptide binding site (Figure 2A). This suggests that binding to the pYFVP peptide causes substantial global conformational changes in the SH2 domain (Figure 3). The binding interaction has an apparently high affinity (and/or slow exchange rate), as the signals underwent intensity changes rather than gradual shifting during the course of titration. For example, Leu77 experienced only a minor perturbation whose magnitude was comparable to the resonance line width. However, its signal still split into two cross-peaks before reaching saturation (Figure 3). Most importantly, the binding interaction seems to involve a 1:2 protein:peptide ratio. This is evident from the data for
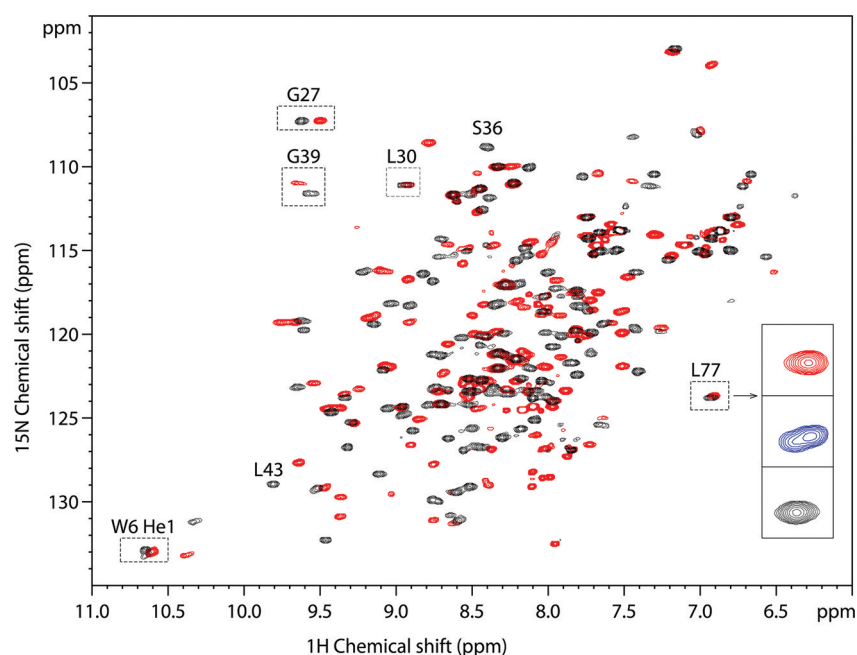
**Figure 3.** Overlap of 2D ¹H−¹⁵N HSQC NMR spectra of the free ¹⁵N-labeled SH2 domain (black) and the protein/peptide mixture at a 1:2.5 ratio (red). The inset is a close-up of L77 signals of the free SH2 protein (black), the 1:1 (molar ratio) protein/peptide mixture (blue), and the 1:2.5 protein/peptide mixture (red). Two peaks of approximately equal intensity are clearly discernible for L77 at the 1:1 protein:peptide ratio despite the small chemical shift difference in the ¹H dimension (∼0.025 ppm).

Leu77, whose signal split into two peaks of roughly equal intensity at a protein:peptide ratio of 1:1. Residue Gly27, which is located in a β-turn region (Figure 2A) and experiences a larger perturbation upon peptide binding, was subsequently analyzed to determine the exact binding ratio. In the absence of peptide ligand, it has a cross-peak at 9.6/107.3 ppm (Figure 4A). Upon addition of the pYFVP peptide, a new peak appeared at 9.5/107.2 ppm, with the concomitant decrease in the intensity of the Gly27 signal of the free protein. The cross-peak at 9.5/107.2 ppm is assigned to Gly27 in the protein−peptide complex (denoted Gly27′ hereafter) on the basis of the parallel NOESY and TOCSY data sets recorded at the end of peptide titration. Quantitative evaluation of their relative peak volumes successfully led to a 1:2 ratio of protein to peptide binding in support of the crystal structure (Table S1 of the Supporting Information).

To gain additional evidence for the two differently bound peptides on a single SH2 domain, we performed a reverse titration experiment in which a specifically ¹³C-labeled peptide (¹³CH₃CO-VIpYFVPLNYRR-NH₂) was titrated with increasing concentrations of the SH2 protein. The free peptide exhibited a single ¹H−¹³C cross-peak at 1.86/21.6 ppm (Figure 4B). Addition of the SH2 protein resulted in a new signal at 1.80/21.5 ppm, whose intensity increased with protein concentration. Unfortunately, the interpretation of the results was somewhat complicated by the observation that the signal for one of the bound N-terminal acetyl groups overlapped with that of the free peptide and that at high SH2 domain protein concentrations (2:1 protein:peptide), all of the cross-peaks (those of the free peptide and the two differently bound peptides) appeared to collapse together, likely because of increased exchange rates. Cooling of the sample to 6 °C improved the quality of the spectrum, which clearly showed two cross-peaks of equal integrals at 1.82/21.3 and 1.78/21.3 ppm. We assign these two cross-peaks to the N-terminal acetyl

groups of the two differentially bound pY peptides. The lack of a significant signal shift of the N-terminal acetyl groups is not unexpected, because the pY-3 residue was not resolved in the crystal structure, presumably due to a lack of interactions with the protein (Figure 1).

Finally, the SH2 domain−pYFVP interaction was examined by 1D ³¹P NMR spectroscopy. The free peptide showed a single resonance at −0.1 ppm (Figure 5A). Upon addition of 0.25 equiv of the N-SH2 domain (1:4 protein:peptide ratio), two new peaks emerged at 0.2 and 1.1 ppm. Integration of the two new peaks as well as the free peptide peak gave a ratio of 1.0:1.1:1.8, in agreement with the 1:2 protein:peptide binding mode. Further addition of the SH2 protein to a 1:1 protein:peptide ratio resulted in the disappearance of the free peptide signal and increased intensities for the peaks at 0.2 and 1.1 ppm (data not shown). As a comparison, binding of a class I ligand (NH₂-VIpYIDVQSYRR-NH₂) to the N-SH2 domain gave only a single resonance at 0.2 ppm, consistent with the formation of a classical 1:1 SH2 domain−pY peptide complex (Figure 5B). The crystal structure shows that the pY side chain of peptide A is engaged in canonical SH2 domain−pY interactions, including electrostatic interactions with ArgβB5 and LysβD6, whereas the pY residue of peptide B is engaged in comparatively fewer interactions with the SH2 domain (e.g., LysBG5). Therefore, the two pY residues are clearly in different chemical environments, giving rise to different ³¹P NMR signals.

**Binding of Peptide B Does Not Require Tyrosine Phosphorylation.** Because the pY side chain of peptide B is exposed to the solvent and appears to make only weak electrostatic interactions with the side chain of LysBG5, we suspected that the phosphate group might not be required for the formation of the 1:2 complex. To test this notion, we immobilized an unphosphorylated peptide [biotin-(miniPEG)₂-RVIYFVPLNR-NH₂ (YFVP peptide)] onto a streptavidin-

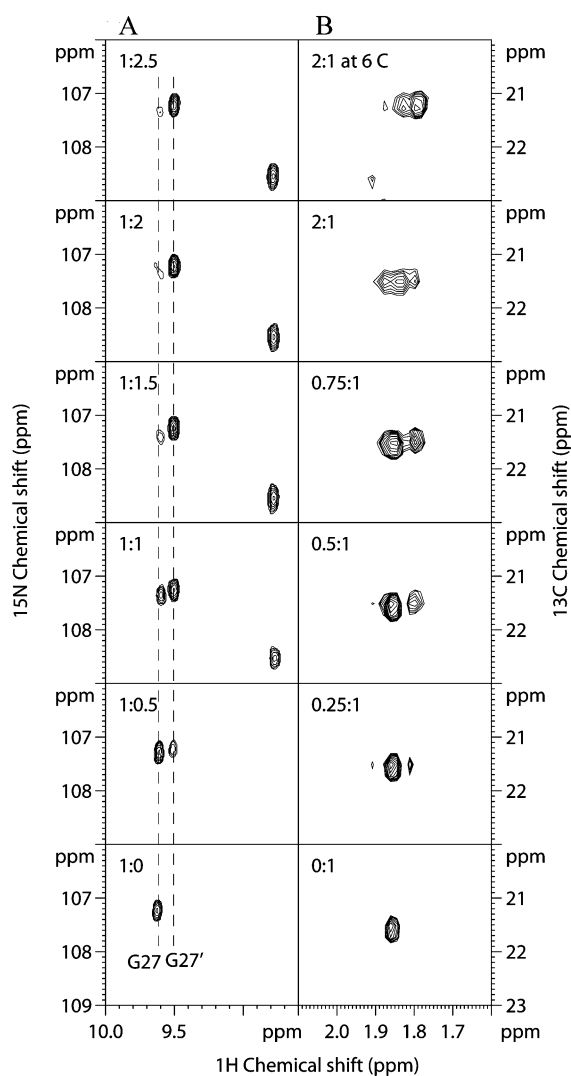**Figure 4.** (A) $^1H-^{15}N$ HSQC spectra of the $^{15}N$-labeled SHP-2 N-SH2 domain (460 $\mu$M) in the absence (1:0 protein:peptide) and presence of increasing concentrations of the pYFVP peptide (at protein:peptide molar ratios of 1:0.5, 1:1, 1:1.5, 1:2, and 1:2.5). The intensity changes of G27 (and G27′) and an unassigned new cross-peak are shown. (B) $^1H-^{13}C$ HSQC spectra of the N-terminally $^{13}C$-labeled pYFVP peptide (200 $\mu$M) in the absence and presence of increasing concentrations of the SHP-2 N-SH2 domain (at protein:peptide ratios of 0:1, 0.25:1, 0.5:1, 0.75:1, and 2:1). All spectra were recorded at room temperature except for that of the top panel in column B, which was recorded at 6 °C.

coated SPR sensorchip and examined its ability to bind the N-SH2 domain in the absence and presence of the pYFVP peptide. As expected, neither the SH2 domain nor the pYFVP peptide alone showed any binding to the surface (Figure 6A and Figure S2 of the Supporting Information). However, when solutions containing both the SH2 domain (at a fixed concentration of 10 $\mu$M) and the pYFVP peptide (1.0−8.4 $\mu$M) were passed over the surface, binding of protein to the surface was observed. Moreover, the amount of binding to the surface increased with pYFVP concentration. A plot of the $RU_{eq}$ values as a function of pYFVP concentration and curve fitting by nonlinear regression analysis gave an apparent $K_D$ value of 1.5 ± 0.2 $\mu$M (Figure 6B). Interestingly, the amount of SH2 domain binding plateaued at ~10 $\mu$M pYFVP peptide and
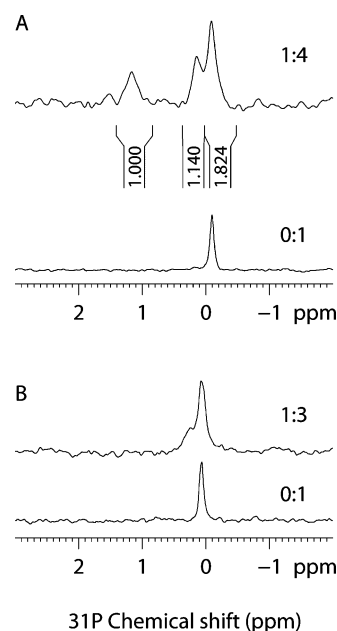


**Figure 5.** (A) 1D $^{31}P$ NMR spectra of class IV peptide NH$_2$-VIpYFVPLNYRR-NH$_2$ (300 $\mu$M) in the presence (1:4 protein:peptide) and absence of 75 $\mu$M SHP-2 N-SH2 domain (0:1) in 50 mM Hepes (pH 7.4) and 150 mM NaCl. The integrated peak area of each peak is shown under the peak. (B) 1D $^{31}P$ NMR spectra of class I peptide NH$_2$-VIpYIDVQSYRR-NH$_2$ (300 $\mu$M) in the presence (1:3) and absence of 100 $\mu$M SHP-2 N-SH2 domain (0:1) in the same buffer as in panel A.



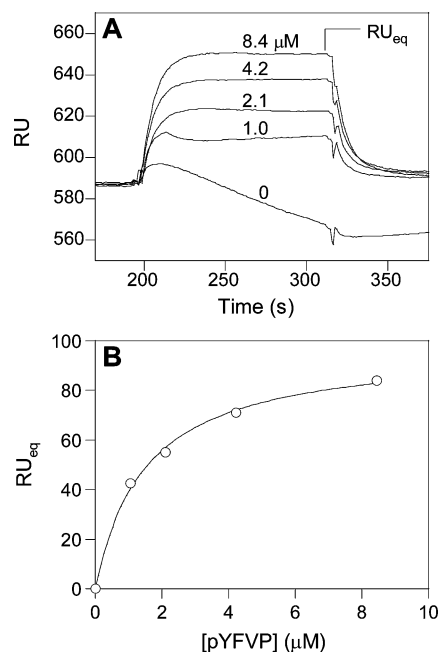**Figure 6.** SPR analysis of the binding of the SHP-2 N-SH2 domain (10 $\mu$M) to immobilized peptide biotin-(miniPEG)$_2$-RVIYFVPLNR-NH$_2$ in the presence of varying concentrations of the pYFVP peptide (0, 1.0, 2.1, 4.2, and 8.4 $\mu$M). (A) Overlaid sensograms at indicated pYFVP concentrations. (B) Plot of $RU_{eq}$ as a function of pYFVP peptide concentration. The curve was fitted to the data according to the equation $RU_{eq} = (RU_{max}[pY])/(K_{Dapp} + [pY])$.

then decreased with a further increase in peptide concentration (i.e., when [pYFVP] > [SH2]); at 60 $\mu$M pYFVP peptide, binding by the SH2 domain to the SPR surface was completely abolished (Figure S2 of the Supporting Information). Finally, mutation of LysBG5 of the SH2 domain to an alanine had little effect on its binding affinity for the immobilized pYFVP peptide (data not shown). The simplest explanation for these observations is that the SHP-2 N-SH2 domain simultaneously bound the pYFVP peptide at the canonical pY peptide-binding site and the YFVP peptide at the binding site for peptide B to form a 1:1:1 heterotrimeric complex. Because peptide B may be either a pY peptide or an unphosphorylated peptide, the presence of excess pYFVP peptide (relative to the SH2 domain) would compete with the immobilized peptide B for binding to the second site on the SH2 domain.

**Dimerization of Peptide pYFVP Increases Binding Affinity.** The antiparallel relationship of peptides A and B in the SH2 domain−pY peptide complex suggests that joining the C-terminus of peptide A with the N-terminus of peptide B (or vice versa) may facilitate the formation of the 1:2 complex and enhance its stability. To test this notion, we designed two tandem pY peptides, RVIpYFVPGGGGGVIpYFVPYR-NH$_2$ (bis-pYFVPG$_5$) and RVIpYFVPGGGGGGVIpYFVPYR-NH$_2$ (bis-pYFVPG$_6$), in which the two pYFVP motifs are joined by flexible pentaglycine and hexaglycine linkers, respectively. SPR analysis of the binding of the N-SH2 domain to the immobilized bis-pYFVPG$_5$ and bis-pYFVPG$_6$ peptides gave apparent $K_D$ values of 0.18 and 0.33 $\mu$M, respectively (Figure S3 of the Supporting Information). Under the same conditions, the SH2 domain bound to the immobilized pYFVP peptide with an apparent $K_D$ value of 0.044 $\mu$M.[6] Because immobilization of the peptides to a surface may facilitate (or interfere with) their dimerization and complicate the quantitative analysis (see Discussion), we next performed a competition assay to determine the binding affinities of these peptides for the N-SH2 domain in solution. We immobilized a class I peptide ligand (pYAQL) onto an SPR sensorchip via its N-terminus and examined the ability of bis-pYFVPG$_5$ and other peptides to compete with the immobilized pY ligand for binding to the SHP-2 N-SH2 domain. An IC$_{50}$ value (concentration at which the amount of SH2 binding is reduced to 50% relative to the control without inhibitor) of 0.65 $\mu$M was obtained for bis-pYFVPG$_5$ (Figure S4 of the Supporting Information and Table 2). As a comparison, the pYAQL

**Table 2. Binding Affinities of the SHP-2 N-SH2 Domain for pY Peptides**

| peptide | IC$_{50}$ ($\mu$M) | $K_D$ ($\mu$M) |
| --- | --- | --- |
| pYAQL | 0.60 ± 0.10 | 0.26 ± 0.02 |
| pYFVP | 2.8 ± 0.8 | 1.2 ± 0.3 |
| bis-pYFVPG$_5$ | 0.65 ± 0.10 | 0.28 ± 0.04 |
| pYFIP | >80 | >35 |

peptide and the monomeric pYFVP peptide had IC$_{50}$ values of 0.60 and 2.8 $\mu$M, respectively. A peptide derived from protein CTLA-4, Ac-QPpYFIPINYRR-NH$_2$, had an IC$_{50}$ value of >80 $\mu$M. On the basis of the previously reported $K_D$ value (0.26 $\mu$M) for the interaction between the SHP-2 N-SH2 domain and the pYAQL peptide,[7] we estimate that peptides pYFVP, bis-pYFVPG$_5$, and QPpYFIP have $K_D$ (or apparent $K_D$) values of 1.2, 0.28, and >35 $\mu$M, respectively. Note that the apparent $K_D$ value of 1.2 $\mu$M for the pYFVP peptide is similar to the $K_D$

value (1.5 $\mu$M) derived from the binding of N-SH2/pYFVP to the YFVP peptide (Figure 6). Thus, the bis-pYFVPG$_5$ peptide binds to the SH2 domain with an ∼4-fold higher affinity than the monomeric pYFVP peptide (or an ∼2-fold enhancement after correction for the higher pY content of the bis-pYFVPG$_5$ peptide).

## ■ DISCUSSION

Among the SH2 domains whose ligand specificities have been well characterized, the N-SH2 domain of SHP-2 is unique in that it recognizes four distinct classes of pY ligands, all of which apparently bind to the same pY-binding site.[6] To understand how the same SH2 domain recognizes vastly different peptide sequences, we investigated the mode of binding of the SHP-2 N-SH2 domain bound to three different classes of peptide ligands by X-ray crystallography. Both class I and III ligands bind to the SH2 domain in a manner very similar to those of numerous other SH2 domain−pY peptide complexes.[9−14] In contrast, the class IV ligand (pYFVP) binds to the SH2 domain as a homodimer. NMR and SPR studies confirmed that the unusual binding mode exists in the solution phase. Further, a database search revealed 32 human proteins that contain one or more putative class IV SHP-2 N-SH2 ligands (Table S2 of the Supporting Information). NMR analysis of five of these putative ligands showed that at least one of them (e.g., pYFLP of TEX10) also bound to the SHP-2 SH2 domain to form a 1:2 protein−peptide complex (Figure S5 of the Supporting Information). We hypothesize that formation of the 1:2 complex with the SHP-2 SH2 domain may be a general property of all class IV ligands. There has been a previous report that the C-terminal SH2 domain of PLCγ binds to a doubly phosphorylated peptide from Syk kinase and forms a 1:1 SH2 domain−pY peptide complex, in which the first pY occupies the canonical pY-binding pocket and the second pY makes additional contacts with the SH2 domain surface.[24] The 1:2 complex in this study is distinct from the previous system in that the two pY peptides (or a pY peptide and a non-pY peptide) in our system may come from two different proteins.

Dimerization of the class IV peptides appears to be required for binding to the SHP-2 N-SH2 domain. For peptides pYFVP and pYFLP, which bind to the SH2 domain tightly, the dissociation rate of the SH2 domain−pY peptide complex is slow enough to allow the NMR signals of the free peptide (or protein) to be resolved from that of the complex. Under all of the conditions tested (with either the peptide or the SH2 domain in excess), only the NMR signals corresponding to the free peptide (or the free protein) and the 1:2 protein−peptide complex were observed. This indicates that the canonical 1:1 peptide−SH2 domain complex is either not formed at all or present at very low concentrations (i.e., below the detection limit of NMR spectroscopy). This in turn suggests that the 1:1 complex, if formed at all, has a substantially lower stability than the 1:2 complex. Peptide dimerization is apparently induced by SH2 domain binding, because in the absence of the SH2 domain the pYFVP peptide showed no detectable binding to the immobilized YFVP peptide ($K_D \gg 60$ $\mu$M). Interestingly, the apparent $K_D$ value of peptide pYFVP as measured by the competition assay in this work (1.2 $\mu$M) is significantly higher than the previously reported $K_D$ value (0.044 $\mu$M), which was determined with the pYFVP peptide immobilized onto an SPR sensorchip.[6] Clearly, immobilization of the pYFVP peptide onto a surface facilitated dimerization of the peptide (because

of high surface density), thereby increasing the stability of the 1:2 SH2 domain−pY peptide complex. The propensity of the pYFVP peptide to dimerize in the presence of the SH2 domain is likely the reason why it was selected from the peptide library in the first place. Consistent with this notion, covalent cross-linking of two pYFVP peptides (e.g., bis-pYFVPG$_5$) resulted in 2−4-fold higher affinity. It is possible that a linker more optimal than pentaglycine may result in even greater binding affinity.

The different interactions between the two bound peptides and the protein may have important implications. The pY side chain of peptide A is engaged in canonical interactions with the pY-binding pocket of the SH2 domain, and binding of peptide A should therefore be phosphorylation-dependent. The pY side chain of peptide B is exposed to the solvent and makes only weak electrostatic interaction with the side chain of LysBG5, suggesting that binding of peptide B should not require tyrosine phosphorylation. Indeed, our results show that the SHP-2 N-SH2 domain can simultaneously bind a pY peptide (e.g., pYFVP) and an unphosphorylated peptide (e.g., YFVP) to form a 1:1:1 heterotrimeric complex. Further, it appears that the two peptides do not need to have the same sequence to form the 1:2 complex (P. H. Tan and D. Pei, unpublished results). In fact, the discovery of the 1:2 complex in which the two peptide ligands are identical is rather fortuitous, due to fact that all of the peptides on each peptide library bead have the same sequence. In the context of proteins, formation of the 1:2 complexes may have two different manifestations. It may form intermolecularly, resulting a trimeric complex involving the SH2 domain, a pY protein, and a third protein (which may or may not be tyrosine-phosphorylated), or intramolecularly, by forming a heterodimer between SHP-2 and a pY protein in which the pY peptide folds into a hairpin structure and binds to the SH2 domain. Obviously, further study is needed to test this hypothesis. It will also be important to determine whether the class I, II, and III ligands are capable of binding to the SHP-2 SH2 domain as dimers (either homo- or heterodimers) or whether other SH2 domains are capable of recognizing peptide dimers.

## ■ ASSOCIATED CONTENT

### Ⓢ Supporting Information

Additional NMR spectra and SPR data showing the SH2 domain−pY peptide binding stoichiometry. This material is available free of charge via the Internet at http://pubs.acs.org.

## ■ AUTHOR INFORMATION

### Corresponding Author

*Department of Chemistry, The Ohio State University, 100 W. 18th Ave., Columbus, OH 43210. Telephone: (614) 688-4068. Fax: (614) 292-1532. E-mail: pei.3@osu.edu.

### Present Address

#National Institutes of Health, National Institute of Child Health and Human Development, 35 Lincoln Drive, Bethesda, MD 20892.

### Funding

## ■ ACKNOWLEDGMENTS

## ■ ABBREVIATIONS

HSQC, heteronuclear single-quantum correlation; PTP, protein tyrosine phosphatase; pY, phosphotyrosine; SH2, Src homology 2; SPR, surface plasmon resonance.

## ■ REFERENCES

(1) Liu, B. A., Jablonowski, K., Raina, M., Arce, M., Pawson, T., and Nash, P. D. (2006) The human and mouse complement of SH2 domain proteins: Establishing the boundaries of phosphotyrosine signaling. *Mol. Cell 22*, 851−868.

(2) Songyang, Z., Shoelson, S. E., Chaudhuri, M., Gish, G., Pawson, T., Haser, W. G., King, F., Roberts, T., Ratnofsky, S., Lechleider, R. J., Neel, B. G., Birge, R. B., Fajardo, J. E., Chou, M. M., Hanafusa, H., Schaffhausen, B., and Cantley, L. C (1993) SH2 domains recognize specific phosphopeptide sequences. *Cell 72*, 767−778.

(3) Huang, H., Li, L., Wu, C., Schlibli, D., Colwill, K., Ma, S., Li, C., Roy, P., Ho, K., Songyang, Z., Pawson, T., Gao, Y., and Li, S. S.-C. (2008) Defining the specificity space of the human Src homology 2 domain. *Mol. Cell. Proteomics 7*, 768−784.

(4) Burshtyn, D. N., Yang, W., Yi, T., and Long, E. O. (1997) A novel phosphotyrosine motif with a critical amino acid at position −2 for the SH3 domain-mediated activation of tyrosine phosphatase SHP-1. *J. Biol. Chem. 272*, 13066−13072.

(5) Poy, F., Yaffe, M. B., Sayos, J., Saxna, K., Morra, M., Sumegi, J., and Eck, M. J. (1999) Crystal structures of the XLP protein SAP reveal a class of SH2 domains with extended, phosphotyrosine-independent sequence recognition. *Mol. Cell 4*, 555−561.

(6) Sweeney, M. C., Wavreille, A.-S., Park, J., Butchar, J., Tridandapani, S., and Pei, D. (2005) Decoding protein-protein interactions through combinatorial chemistry: Sequence specificity of SHP-1, SHP-2, and SHIP SH2 domains. *Biochemistry 44*, 14932−14947.

(7) Imhof, D., Wavreille, A.-S., May, A., Zacharias, M., Tridandapani, S., and Pei, D. (2006) Sequence specificity of SHP-1 and SHP-2 Src Homology 2 domains: Critical roles of residues beyond the pY+3 position. *J. Biol. Chem. 281*, 20271−20282.

(8) Kaneko, T., Huang, H., Zhao, B., Li, L., Liu, H., Voss, C. K., Wu, C., Schiller, M. R., and Li, S. S.-C. (2010) Loops govern SH2 domain specificity by controlling access to binding pockets. *Sci. Signaling 3*, ra34.

(9) Waksman, G., Kominos, D., Robertson, S. C., Pant, N., Baltimore, D., Birge, R. B., Cowburn, D., Hanafusa, H., Mayer, B. J., Overduin, M., Resh, M. D., Rios, C. B., Silverman, L., and Kuriyan, J. (1992) Crystal structure of the phosphotyrosine recognition domain SH2 of v-Src complexed with tyrosine-phosphorylated peptides. *Nature 358*, 646−653.

(10) Waksman, G., Shoelson, S. E., Pant, N., Cowburn, D., and Kuriyan, J. (1993) Binding of a high-affinity phosphotyrosyl peptide to the Src SH2 domain: Crystal structures of the complexed and peptide-free forms. *Cell 72*, 779−790.

(11) Eck, M., Shoelson, S. E., and Harrison, S. C. (1993) Recognition of a high affinity phosphotyrosyl peptide by the Src homology 2 domain of p56^lck. *Nature 362*, 87−91.

(12) Lee, C., Kominos, D., Jacques, S., Margolis, B., Schlessinger, J., Shoelson, S. E., and Kuriyan, J. (1994) Crystal structures of peptide complexes of the amino-terminal SH2 domain of the Syp tyrosine phosphatase. *Structure 2*, 423−438.

(13) Pascal, S. M., Singer, A. U., Gish, G., Yamazaki, T., Shoelson, S. E., Pawson, T., Kay, L. E., and Forman-Kay, J. D. (1994) Nuclear-

magnetic-resonance structure of an SH2 domain of phospholipase C-γ-1 complexed with a high-affinity binding peptide. *Cell 77*, 461−472.

(14) Xu, R. X., Word, J. M., Davis, D. G., Rink, M. J., Willard, D. H., and Gampe, R. T. (1995) Solution structure of the human pp60(c-Src) SH2 domain complexed with a phosphorylated tyrosine pentapeptide. *Biochemistry 34*, 2107−2121.

(15) Neel, B. G., Gu, H., and Pao, L. (2003) The "Shp"ing news: SH2 domain-containing tyrosine phosphatases in cell signaling. *Trends Biochem. Sci. 28*, 284−293.

(16) Hof, P., Pluskey, S., Dhe-Paganon, S., Eck, M. J., and Shoelson, S. E. (1998) Crystal Structure of the Tyrosine Phosphatase SHP-2. *Cell 92*, 441−450.

(17) Lechleider, R. J., Sugimoto, S., Bennett, A. M., Kashishian, A. S., Cooper, J. A., Shoelson, S. E., Walsh, C. T., and Neel, B. G. (1993) Activation of the SH2-containing phosphotyrosine phosphatase SH-PTP2 by its binding-site, phosphotyrosine-1009, on the human platelet-derived growth-factor receptor-β. *J. Biol. Chem. 268*, 21478−21481.

(18) Pluskey, S., Wandless, T. J., Walsh, C. T., and Shoelson, S. E. (1995) Potent stimulation of SH-PTP2 phosphatase activity by simultaneous occupancy of both SH2 domains. *J. Biol. Chem. 270*, 2897−2900.

(19) Otwinowski, Z., and Minor, W. (1997) Processing of X-ray diffraction data collected in oscillation mode. *Methods Enzymol. 276*, 307−326.

(20) Collaborative Computational Project, Number 4 (1994) The CCP4 Suite: Programs for Protein Crystallography. *Acta Crystallogr. D50*, 760−763.

(21) Emsley, P., Lohkamp, B., Scott, W. G., and Cowtan, K. (2010) Features and development of Coot. *Acta Crystallogr. D66*, 486−501.

(22) Holm, L., and Rosenström, P. (2010) Dali server: Conservation mapping in 3D. *Nucleic Acids Res. 38*, W545−W549.

(23) Thornton, K. H., Mueller, W. T., McConnell, P., Zhu, G., Saltiel, A. R., and Thanabal, V. (1996) Nuclear magnetic resonance solution structure of the growth factor receptor-bound protein 2 Src homology 2 domain. *Biochemistry 35*, 11852−11864.

(24) Groesch, T. D., Zhou, F., Mattila, S., Geahlen, R. L., and Post, C. B. (2006) Structural basis for the requirement of two phosphotyrosine residues in signaling mediated by Syk tyrosine kinase. *J. Mol. Biol. 356*, 1222−1236.